

Organic light-emitting transistors using concentric source/drain electrodes on a molecular adhesion layer

Clara Santato

CNR, ISMN, Via Gobetti 101, 40129 Bologna, Italy

Fabio Cicoira^{a)}

CNR, ISMN, Via Gobetti 101, 40129 Bologna, Italy and INRS-EMT, Université du Québec, 1650 Boulevard Lionel Boulet, J3X 1S2 Varennes (QC), Canada

Piero Cosseddu and Annalisa Bonfiglio

DIEE, Università di Cagliari, Italy and INFN-S3, Modena, Italy

Pierluigi Bellutti

ITC, IRST, Microsystem Division, Via Sommarive 18, I-38050 Povo (Trento), Italy

Michele Muccini and Roberto Zamboni

CNR, ISMN, Via Gobetti 101, 40129 Bologna, Italy

Federico Rosei

INRS-EMT, Université du Québec, 1650 Boulevard Lionel Boulet, J3X 1S2 Varennes (QC), Canada

Arnaud Mantoux and Pascal Doppelt

Centre d'Etude de Chimie Métallurgique, CNRS 15 Rue G. Urbain, F-94407 Vitry sur Seine, France

(Received 16 December 2005; accepted 13 March 2006; published online 20 April 2006)

Bottom-contact tetracene light-emitting transistors employing a mercaptosilane derivative self-assembled monolayer as adhesive between gold concentric interdigitated source/drain electrodes and SiO₂ gate dielectric are described. Devices that employ the mercaptosilane adhesive have a higher mobility and electroluminescence compared to those employing a standard metallic adhesive. This is rationalized in terms of the large, well interconnected grains found in tetracene films deposited on substrates using the mercaptosilane adhesive. Our work represents a step forward in the understanding of physical processes at semiconductor/metal and semiconductor/dielectric interfaces in organic devices. © 2006 American Institute of Physics. [DOI: 10.1063/1.2193468]

Electrical and optoelectronic devices such as field-effect transistors (FETs), light-emitting diodes, and photovoltaic cells based on organic active materials are of great interest for technological applications as well as for fundamental studies.^{1,2} Recently, another class of organic optoelectronic devices has been demonstrated, i.e., organic light-emitting transistors (OLETs).^{3–10} OLETs are appealing since they integrate the switching function of a transistor with light emission. Moreover, they are excellent test systems to investigate physical processes such as charge injection, transport, and electroluminescence in organic films.

Bottom contact organic FETs (OFETs) and OLETs (i.e., organic active film deposited on a prepatterned substrate) are suitable for fundamental studies since this geometry ensures high injection efficiency and prevents reaction between the metal and the organic film.¹¹ OFETs and OLETs usually employ Au electrodes on a SiO₂ gate dielectric. The poor adhesion of Au on SiO₂ requires the use of a metal thin film as adhesion layer. This introduces a second organic/metal interface along the electrode wall and results in an increased electrode thickness, influencing both the growth of the organic film and the physical processes in the device. To avoid the metal adhesion layer, a low-cost and straightforward approach can be used, based on a self-assembled monolayer (SAM) of [HS-(CH₂)₃-Si-(OCH₃)₃], 3-mercaptopropyltrimethyloxysilane (MPTMS).^{12–15} The application of MPTMS SAMs to OLETs may provide a better understanding of

physical processes at the semiconductor/metal and semiconductor/dielectric interfaces.

Here, we report the fabrication and characterization of bottom-contact tetracene OLETs employing concentric Au interdigitated source and drain (S/D) electrodes, where a MPTMS SAM was used to promote Au adhesion on SiO₂. A dedicated interdigitated electrode layout was designed. This geometry is suitable for OLETs as it maximizes the electroluminescence intensity. The concentric geometry allows to circumvent parasitic currents due to the unpatterned semiconducting film,¹⁶ permitting an unambiguous interpretation of the optoelectronic characteristics.

Heavily doped (0.01–0.02 Ω cm) *n*-Si wafers (gate electrode), covered with a thermal SiO₂ layer (gate dielectric), were silylated by MPTMS.¹⁷ The reaction was performed in the gas phase to achieve a reproducible growth of the SAM.¹⁸ Silylation was followed by deposition of a 30 nm thick Au film and by a photolithographic definition of the S/D electrodes. For comparison, standard substrates using the same layout but having a metal film as adhesion layer were fabricated.¹⁹ Electrode definition was achieved via chemical wet etching.²⁰ Hereafter, electrodes employing MPTMS as adhesion layer will be indicated as Au/MPTMS, and those employing Cr as Au/Cr. Tetracene (TCI, 98%) was used as source material. The deposition system and the apparatus for optoelectronic measurements have been described elsewhere.²¹

Figure 1(a) shows the layout of an interdigitated concentric S/D Au electrodes. Figures 1(b) and 1(c) display scan-

^{a)}Electronic mail: cicoira@emt.inrs.ca

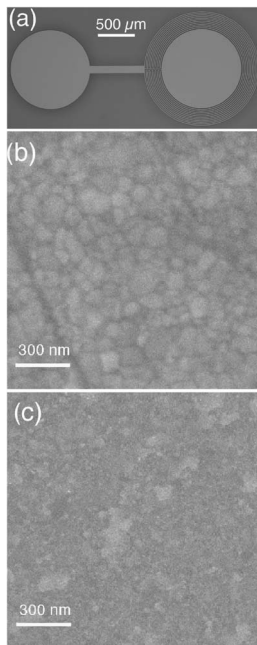


FIG. 1. (Color online) Interdigitated concentric Au source and drain electrodes with $W/L=18\,800/40\ \mu\text{m}/\mu\text{m}$ (a). Two more geometries were used with $W/L=41\,800/6$ and $41\,000/10\ \mu\text{m}/\mu\text{m}$. SEM images of Au/MPTMS (b) and Au/Cr (c) electrodes acquired using a JEOL 6100 SEM and a LEO 1530 SEM (equipped with a Gemini field emission column).

ning electron microscopy (SEM) images of the surfaces of Au/MPTMS and Au/Cr electrodes. The films have different morphologies. Au/Cr shows grains with a typical size of 100 nm. In the case of Au/MPTMS the grains have an inhomogeneous size distribution. Surface enhanced Raman spectroscopy had previously shown that, on SiO_2 , Au/MPTMS films exhibit a reduced surface roughness compared to Au/Cr films.²²

Figures 2(a) and 2(b) display optoelectronic output characteristics of tetracene LETs using Au/MPTMS and Au/Cr electrodes. The plots report drain-source current (I_{ds}) and electroluminescence (EL), vs drain-source voltage (V_{ds}) for increasing gate-source voltages (V_{gs}). The hole FET mobility, μ , was calculated at the saturation using the following relationship:²³

$$|I_{ds,\text{sat}}| = \frac{W}{2L} \mu C_i (V_{gs} - V_T)^2,$$

where W is the channel width, L is the channel length, C_i is the capacitance per unit area ($1.7 \times 10^{-8}\ \text{F cm}^{-2}$ for 190 nm thick SiO_2), and V_T is the threshold voltage. V_T ranges between -7 and $-10\ \text{V}$ for both kind of devices. The MPTMS adhesion layer leads to a higher mobility. The highest μ values observed from several samples, prepared in different deposition runs, were about 1×10^{-2} in LETs employing Au/MPTMS electrodes and $1 \times 10^{-3}\ \text{cm}^2/\text{Vs}$ in those employing Au/Cr. The ratio $I_{\text{on}}/I_{\text{off}}$ is typically 10^6 for both kind of devices. Figures 2(a) and 2(b) reveal that, under the same bias ($V_{ds}=-40$ and $V_{gs}=-30\ \text{V}$), the EL signal is one order of magnitude more intense for LETs using Au/MPTMS electrodes compared to Au/Cr. In addition, with MPTMS, the EL generation requires lower $|V_{gs}|$ and $|V_{ds}|$. Figure 2(c) displays the linear dependence of the width normalized device resistance (RW) on the channel length (L) for Au/Cr and Au/MPTMS substrates. R is deduced from the inverse slope of the output curves in the linear region (at

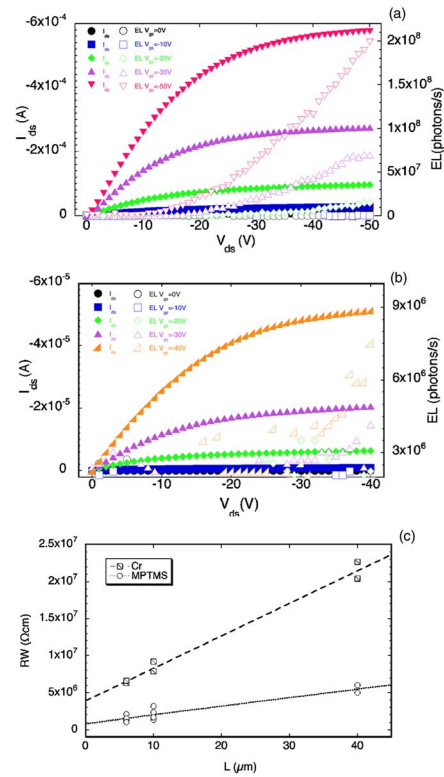


FIG. 2. (Color online) Optoelectronic output characteristics of tetracene LETs employing Au/MPTMS (a) and Au/Cr (b) electrodes. I_{ds} on the left y axis and EL on the right y axis vs V_{ds} at increasing V_{gs} . $W/L=41\,800/6\ \mu\text{m}/\mu\text{m}$. (c) RW as a function of L for devices fabricated on Au/Cr and Au/MPTMS substrates. The correlation coefficient is 0.99 for Au/Cr and 0.94 for Au/MPTMS. $W/L=41\,800/6$, $41\,000/10$, and $18\,800/40\ \mu\text{m}/\mu\text{m}$. Deposition flux of the active films: $4\ \text{\AA}/\text{s}$. Nominal thickness: 30 nm.

$V_{gs}=-40\ \text{V}$). The intercept with the y axis allows the evaluation of the specific contact resistance,²⁴ which is $\approx 2\ \text{M}\Omega\ \text{cm}$ for Au/Cr and $\approx 0.5\ \text{M}\Omega\ \text{cm}$ for Au/MPTMS. This result shows that the use of the molecular adhesion layer leads to a decrease of the contact resistance, in agreement with the literature.²⁵

Figures 3(a) and 3(b) display $6 \times 6\ \mu\text{m}^2$ atomic force microscopy (AFM) images of tetracene films deposited on substrates patterned with Au/MPTMS and Au/Cr electrodes, respectively. The corresponding line profiles at the electrode step are shown in the insets. The two substrates lead to significantly different growth scenarios. As shown in the histograms reported in Figs. 3(c) and 3(d), in the channel region the grain size is larger and the grain size distribution is less homogeneous for films deposited on substrates patterned with Au/MPTMS electrodes. The grain perimeter is about 800 nm for substrates patterned with Au/Cr and about 2000 nm for those patterned with Au/MPTMS. On such substrates, films are more continuous at the electrode interface, with better interconnected grains, because of the lower electrode step. The images reported in Figs. 3(a) and 3(b) show films grown during the same deposition run, thus the different morphologies are related to substrate properties. To gain insight into this aspect, we measured the root mean square (rms) roughness in the channel region of the two SiO_2 substrates. AFM measurements reveal that SiO_2 substrates patterned with Au/MPTMS have a rms roughness of 0.2 nm whereas those with Au/Cr have a higher rms roughness, i.e. 0.6 nm. This higher value may be attributed to the local re-

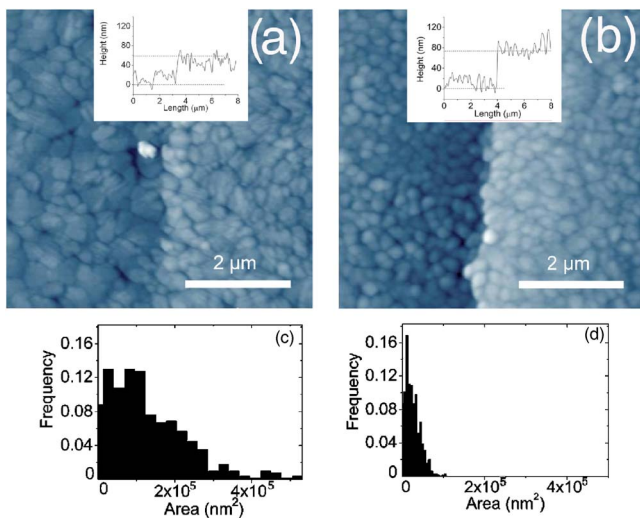


FIG. 3. (Color online) $6 \times 6 \mu\text{m}^2$ AFM images of tetracene films grown on substrates patterned with Au/MPTMS (a) and Au/Cr (b) electrodes. The left panels show film morphology in the channel (SiO_2) and the right panels show film morphology on the contacts (Au). In the inset of each figure is reported the corresponding line profile at the electrode step. The images were acquired with a Solver Pro AFM (NT-MDT) in semicontact mode using NSG-01 Si cantilevers. Histograms showing the grain size distribution in the channel for tetracene films grown on substrates patterned with Au/MPTMS (c) and Au/Cr (d) electrodes.

dox reaction of Cr on SiO_2 that occurs during annealing. The surface roughness of the SiO_2 dielectric strongly influences the morphology of the organic film. Smoother surfaces favor the nucleation of larger islands, leading to films composed of larger grains. This implies a lower number of grain boundaries, which act as carrier traps that contribute to reduce the FET mobility.^{26,27} The larger size of the tetracene grains together with their improved interconnection at the electrode interface should increase the number of carriers injected and transported through the transistor channel. This would in turn increase the number of excitons available to emit light after electron-hole recombination. This is a plausible explanation of the increased EL intensity observed when MPTMS is employed as adhesion layer.

In conclusion, we fabricated OLETs employing a MPTMS SAM adhesion layer between SiO_2 gate dielectric and Au electrodes by a straightforward and low-cost method. To circumvent parasitic currents and to maximize the EL signal, we used concentric and interdigitated Au electrodes. The MPTMS adhesion layer, enabling the minimization of electrode thickness, reduces the influence of the prepatterned substrate on the growth of the organic active film, thus leading to better interconnected tetracene grains at the semiconductor/electrode interface. Moreover, the use of the molecular adhesion layer results in a smoother gate dielectric surface leading to increased tetracene grain size. Tetracene LETs employing a MPTMS SAM as adhesion layer exhibit significantly higher hole mobility and EL intensity, together with lower contact resistance, compared to standard substrates.

The authors acknowledge L. Lorenzelli (ITC) for mask design, A. Lui (ITC) for SEM imaging, P. Maccagnani (CNR), A. Bentley (Purdue Univ.), J. A. Miwa, and F. Vetrone (INRS) for critical reading of the manuscript, projects FIRB-RBNE033KMA and FIRB-RBAUOITH2A_002 for funding. F.C. acknowledges the CBIE for a post-doctoral fellowship. F.R. is grateful to FQRNT and the Canada Research Chairs program for salary support.

- ¹G. Malliaras and R. Friend, *Phys. Today* **58**, 53 (2005).
- ²S. R. Forrest, *Nature (London)* **428**, 911 (2004).
- ³A. Hepp, H. Heil, W. Weise, M. Ahles, R. Schmechel, and H. von Seggern, *Phys. Rev. Lett.* **91**, 157406 (2003).
- ⁴C. Rost, S. Karg, W. Riess, M. A. Loi, M. Murgia, and M. Muccini, *Appl. Phys. Lett.* **85**, 1613 (2004).
- ⁵C. Santato, I. Manunza, A. Bonfiglio, F. Cicoira, P. Cosseddu, R. Zamboni, and M. Muccini, *Appl. Phys. Lett.* **86**, 141106 (2005).
- ⁶T. Sakanoue, E. Fujiwara, R. Yamada, and H. Tada, *Appl. Phys. Lett.* **84**, 3037 (2004).
- ⁷T. Oyamada, H. Sasabe, C. Adachi, S. Okuyama, N. Shimoji, and K. Matsushige, *Appl. Phys. Lett.* **86**, 093505 (2005).
- ⁸F. Cicoira, C. Santato, M. Melucci, L. Favaretto, M. Gazzano, M. Muccini, and G. Barbarella, *Adv. Mater.* **18**, 169 (2006).
- ⁹J. S. Swensen, C. Soci, and A. J. Heeger, *Appl. Phys. Lett.* **87**, 253511 (2005).
- ¹⁰J. Zaumseil, R. H. Friend, and H. Sirringhaus, *Nat. Mater.* **5**, 69 (2006).
- ¹¹Y. Shen, A. R. Hosseini, M. H. Wong, and G. G. Malliaras, *ChemPhysChem* **5**, 16 (2004).
- ¹²C. A. Goss, D. H. Charych, and M. Majda, *Anal. Chem.* **63**, 85 (1991).
- ¹³I. Doron-Mor, Z. Barkay, N. Filip-Granit, A. Vaskevich, and I. Rubinstein, *Chem. Mater.* **16**, 3476 (2004).
- ¹⁴Y.-L. Loo, R. L. Willett, K. W. Baldwin, and J. A. Rogers, *J. Am. Chem. Soc.* **124**, 7654 (2002).
- ¹⁵MPTMS reacts with the silanol groups at the SiO_2 surface via the $-\text{OCH}_3$ functionalities by the formation of Si-O-Si bonds and the elimination of CH_3OH . This results in a -SH terminated surface with a chemical affinity for Au, which enables the deposition of very thin Au layers.
- ¹⁶E. J. Meijer, C. Detcheverry, P. J. Baesjou, E. van Veenendaal, D. M. de Leeuw, and T. M. Klapwijk, *J. Appl. Phys.* **93**, 4831 (2003).
- ¹⁷P. Doppelt, N. Semaltianos, C. Deville Cavellin, J. L. Pastol, and D. Ballutaud, *Microelectron. Eng.* **76**, 113 (2004).
- ¹⁸P. Schwartz, F. Schreiber, P. Eisenberg, and G. Scoles, *Surf. Sci.* **423**, 208 (1999).
- ¹⁹Electrodes were fabricated using a 6 nm thick Cr layer, followed by a 55 nm thick Au film. The higher Au thickness was required to prevent interdiffusion of Cr and Au occurring during the 30 min annealing in N_2 at 190°C performed to stabilize the Au/Cr contact.
- ²⁰A solution of $\text{Na}_2\text{S}_2\text{O}_3$, $\text{CS}(\text{NH}_2)_2$, and $\text{K}_3[\text{Fe}(\text{CN})_6]$ was used for the Au etch and a solution of $(\text{NH}_4)_2\text{Ce}(\text{NO}_3)_6$ and acetic acid for the Cr etch. Prior to organic film deposition, the substrates were cleaned by an O_2 plasma (100 W for 5 min), which ensures the removal of traces of MPTMS.
- ²¹F. Cicoira, C. Santato, F. Dinelli, M. Murgia, M. A. Loi, F. Biscarini, R. Zamboni, P. Heremans, and M. Muccini, *Adv. Funct. Mater.* **15**, 375 (2005).
- ²²P. A. Mosier-Boss and S. H. Lieberman, *Appl. Spectrosc.* **53**, 862 (1999).
- ²³S. M. Sze, *Physics of Semiconductor Devices*, 2nd ed. (Wiley, New York, 1981).
- ²⁴G. B. Blanchet, C. R. Fincher, M. Lefenfeld, and J. A. Rogers, *Appl. Phys. Lett.* **84**, 296 (2004).
- ²⁵N. Yoneya, M. Noda, N. Hirai, K. Nomoto, M. Wada, and J. Kasahara, *Appl. Phys. Lett.* **85**, 4663 (2004).
- ²⁶S. E. Fritz, T. W. Kelley, and C. D. Frisbie, *J. Phys. Chem. B* **109**, 10574 (2005).
- ²⁷N. Karl, in *Organic Electronic Materials*, edited by R. Farchioni and G. Grosso (Springer, Berlin, 2001).